ISSN 1330-3651 (Print), ISSN 1848-6339 (Online)
Received: 24 May 2025; Accepted: 17 December 2025

https://doi.org/10.17559/TV-20250524002691
Original scientific paper

Fuzzy-Integrated Direct Model Predictive Power Control for Enhanced Stability in Renewable Energy Systems

P. SAI SAMPATH KUMAR*, P. SURESH, D. LENINE

Abstract: This paper presents a novel Direct Model Predictive Power Controller (DMPPC) designed to address voltage fluctuations and power quality issues arising from variable load demands and the intermittent behavior of renewable energy sources (RES). The proposed control framework incorporates a bidirectional DC-DC converter integrated with a Battery Energy Storage (BES) system to manage power flow and stabilize the DC bus voltage. A fuzzy logic-based decision-making mechanism dynamically optimizes energy exchange, enhancing system adaptability across varying operating conditions. Furthermore, the AC/DC interlinking converter is regulated in real-time based on both grid constraints and the BES state of charge, enabling efficient energy exchange and stable AC voltage support. Unlike traditional layered control structures, the DMPPC introduces an enhanced cost function that fuses predictive control with fuzzy objectives, thereby offering superior resilience to external disturbances and system nonlinearities. MATLAB/Simulink-based simulations were conducted under diverse loading scenarios, including linear and non-linear loads. Results confirm the superior performance of the proposed controller in minimizing Total Harmonic Distortion (THD), improving dynamic response, and increasing energy conversion efficiency, when compared to conventional control methods such as Sliding Mode Control (SMC). By effectively mitigating voltage instabilities and enhancing power quality, the DMPPC facilitates reliable and robust integration of RES into smart utility grids. These findings affirm its potential for advancing the management and control of renewable-powered hybrid energy systems.

Keywords: battery energy storage (BES); direct model predictive power control (DMPPC); fuzzy decision-making; renewable energy systems (RES); total harmonic distortion (THD)

1 INTRODUCTION

In larger grid systems, possible limitations are higher computational demands, challenges in data management, slower simulation performance, and scalability issues in precisely capturing diverse dynamic behaviors across interconnected networks. In recent years, there has been a growing interest in grid-tied solar and wind turbines, along with other renewable energy source (RES)-based generation technologies. Distributed generation systems increasingly rely on grid-connected inverters as a fundamental component for efficient operation. Consequently, the performance and effectiveness of these inverters are largely determined by the adopted control strategies [1, 2]. Hybrid configurations, which integrate multiple renewable energy sources with energy storage systems, have emerged as a promising solution for enhancing both the technical and economic performance of power generation systems. These systems offer improved reliability, flexibility, and energy management capabilities. Whether in standalone (off-grid) or grid-connected modes, hybrid systems that combine wind, photovoltaic (PV), and battery storage are considered highly desirable and cost-effective. Their ability to ensure stable power supply, mitigate intermittency, and provide load balancing makes them particularly suitable for modern energy needs and smart grid integration.

Due to the increasing ubiquity of DC-built sources with micro grids and the need to take into consideration an era older ac power structures, importance in hybrid ac/dc micro-grids has begun to grow rapidly in recent years. Given their ability to efficiently handle the stochastic nature of both distributed generation (DG) as well as energy via RES, such as wind and photovoltaic energy, microgrids represent the most viable options for integrating DG and RES into power distribution networks. In addition, microgrids provide reduced transmission and distribution costs, greater dependability, and decreased energy losses [3, 4].

These microgrids usually use PID controllers to govern the interlinking AC/DC circuits and DC to DC converters through cascading inner current and outer voltage looping connections. The bi-directional DC to DC configuration retains the DC side voltage, and the primary interlinking AC/DC systems have been modified to provide uniform frequency along with voltage whereas the AC sub grid operates in islanded mode [5, 6].

MATLAB/Simulink is used for its strong toolboxes and accurate modeling. The model is validated by comparing with benchmarks, checking sensitivity, and matching results from existing literature. Hence, MATLAB/Simulink is adopted as the simulation platform paper to ensure reliable modeling, analysis, and validation of the system performance.

2 RELATED WORKS

The main sources of problems with electrical power quality associated with the hybrid PV/wind/battery power system are harmonic generations, voltage changes, and frequency swings. Actually, the main sources of harmonics are non-linear loads and non-linear components like power converters. Furthermore, the primary causes of variations in frequency and voltage are modifications in methodical issue conditions and network disruptions. Microgrid applications have improved things, but there are still a lot of technical issues that researchers in electrical engineering need to concentrate on [7, 8]. Using the grid-interfaced converter, the microgrid is expected to meet the operational requirements of several more power electronic devices. This might slash the overall cost as well as complexity of the network. Several guidelines are proposed to regulate the microgrid application. Power quality, specifically the current harmonic distortion, is one of the indicators.

One way to address these issues is to design the proper control regulations for power converters in hybrid systems. Storage units are mainly introduced to the energy mix to deal with such stability concerns, though they are also used

as spinning reserves. They help the PCC adjust voltage and frequency and store energy generated by solar and wind farms during off-peak hours. Controlling the working of hybrid AC/DC grids could be complicated by the timescale variance among sluggish AC responses and quicker DC responses [9]. Unsuited control design can result in poor transient operation and oscillations. Therefore, it is necessary to develop systematic design and analysis methodologies.

Technology improvements in processing power have made it possible to apply complex control techniques. Model predictive control (MPC) thereby works with systems that have precise mathematical models, and is one such promising control technique [10, 11]. Since a standard VSC could be simulated through a linear mathematical representation, MPC control is a better choice. Conversely, though a fuzzy control, which is built on fuzzy based decision making (FDM), does not require a mathematical model because control objectives and commands are defined using human knowledge [12-15], most real-life situations are hard to model numerically and instead rely on estimates or predictions due to wide changes in parameters and a lack of necessary data.

In order to enrich the transient performance of the PV farm, the fuzzy depended gain scheduling sequence used by the PID controller has been described in [16, 17]. Fuzzy-MPC control integrates FDM and conventional MPC to address complicated and fluctuating control systems. Numerous conventional control techniques, such as PID controllers, have been studied over the years for voltage control [18, 19]. The majorityof these advanced control methods involve space vector modulation that is based on three dimensions, which is a laborious, complex, and challenging process to perform [20].

When designing the goal-oriented features for MPC alongside various scenarios FDM or in systems with non-linear models, fuzzy-based MPC controllers may be employed [21, 22]. The authors of [23] suggest an improved duty cycle modulation procedure for fuzzy logic modelled duty cycle modulation (MPDPC). Some systems require unique control upon the components for the objective function; subsequently the extent of influence can vary dynamically through response to human intelligence based on experience[24-26].

The research gap lies in the lack of robust, adaptive control strategies capable of simultaneously handling the non-linearities, dynamic disturbances, and hybrid nature of PV/wind/battery energy systems in grid-connected microgrids. Existing conventional control methods like PID and traditional MPC are limited by their dependence on linear models, insufficient adaptability to rapid system variations, and high implementation complexity, especially under variable load and grid conditions. Additionally, the integration of bidirectional energy flow in BESS with efficient control remains underexplored. This study addresses this gap by proposing a fuzzy-based Direct Model Predictive Power Control (DMPPC) system for enhanced reliability, adaptability, and power quality.

3 DESIGN PROCEDURES OF THE PROPOSED CONTROLLERS

The key proposals of this article are the application of FDM predictive control over grid-connected converter control as well as the automatic control of the converter to regulate a BESS's bi-directional flow of power in accordance with dynamic system circumstances. A fuzzy-DMPPC mechanism has been suggested and its performance is shown methodically via the MATLAB Simulink platform. The block diagram of the proposed system is shown in Fig. 1.

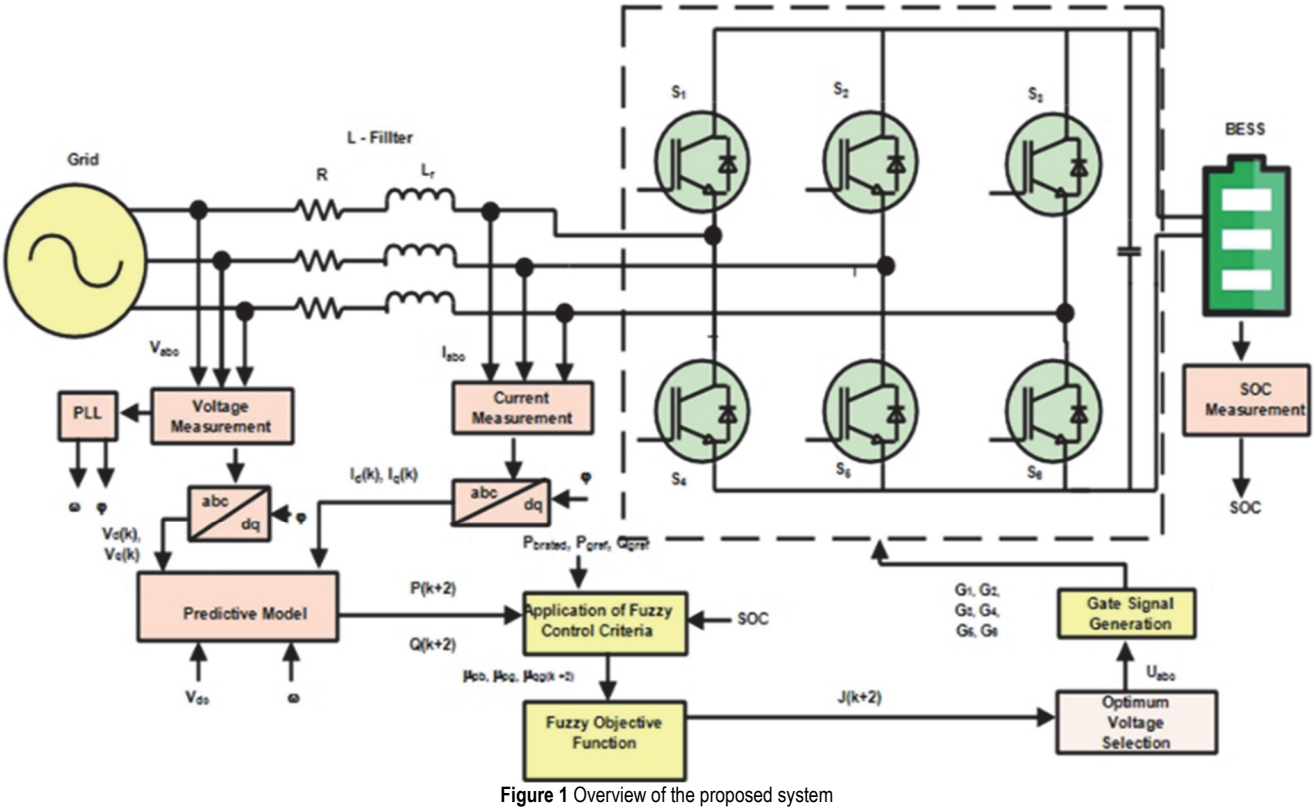

Figure 1 Overview of the proposed system

3.1 Fuzzy Control Algorithm

The significance of fuzzy control lies in its ability to incorporate human understanding concepts as control rules over an array of rules. These arrays of rules are typically specified by a design engineer or operator with system experience. The fuzzy logic controller uses triangular membership functions for inputs and outputs. SOC is split into low (0-30%), medium (30-70%), and high (70-100%). RES fluctuation is also low, medium, or high. Nine simple IF-THEN rules guide charging and discharging. The Mamdani method with centroid defuzzification ensures smooth, adaptive control.

The following are the control measures defined by fuzzy DPMPC. Appropriate control over power is required to maximize the benefits and prolong the life of expensive BESS. This leads to the establishment of a minimum SOC threshold λ_1 for battery discharge. Reactive power might be released as soon as state of charge attains λ_1 after the battery starts to charge when the SOC magnitude attains λ_2. The battery shall be utilized readily for grid environments once it attains a SOC magnitude of λ_3.

Eqs. (1) to (3) is the expression of the error functions. e_p, e_q, along with e_b represents error cost of real, reactive power, in addition to battery power. Furthermore, its appropriate membership functions, μ_{pg}, μ_{qg}, along with μ_{pb}, are shown in exponential form, as given in Eq. (4). The membership deviation with reference towards error functions of true, power, in addition to battery power is adjusted using normalization variables *Kp*, *Kq*, and *Kb*. The exponential model is chosen because it is more likely to affect the objective function, even though the error is tiny. The entire of these uncertain criteria should be defined by the design engineer, along with parameter settings that align with the system's requirements and specifications for performance. The design requirements for membership functions have been satisfied, and as shown in Fig. 2 of this article, the proper SOC range to control BESS's operation is determined. The basic block diagram of the suggested fuzzy-based MPC control structure is displayed in Fig. 3.

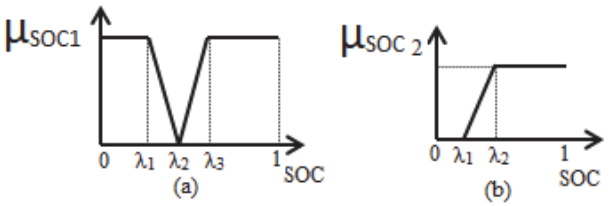

Figure 2 SOC limits: (a) Reactive power and (b) Active power

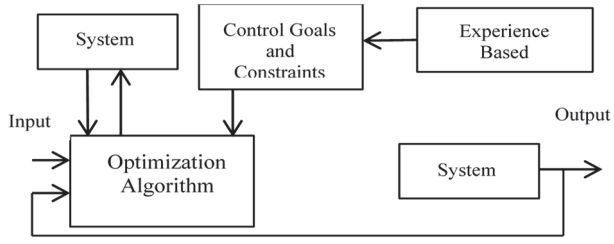

Figure 3 Fundamental layout of the suggested FLC-Based MPC

$$E_{rp}\left(j+2\right)=P\left(j+2\right)-\left(P_{g_{ref}}\cdot\gamma_{SOC1}\right) \tag{1}$$

$$E_{rq}\left(j+2\right)=Q\left(j+2\right)-\left(Q_{g_{ref}}\cdot\gamma_{SOC2}\right) \tag{2}$$

$$E_{rb}\left(j+2\right)=P\left(j+2\right)-\left(P_{b\_rat}\cdot\gamma_{SOC1}\right) \tag{3}$$

$$\mu_{p_g,q_g,p_b}=\begin{cases}\exp\left(\dfrac{e_{p,q,b}\left(j+2\right)}{K_{p,q,b}}\right) & -\infty<e\left(j+2\right)<0\\ exp\left(-\dfrac{e_{p,q,b}\left(j+2\right)}{K_{p,q,b}}\right) & 0\le e\left(j+2\right)<\infty\end{cases} \tag{4}$$

3.2 DMPPC Control Algorithm

Clarke & Park transformations are used to convert the network voltage expressions to synchronous reference frame in order to overcome the control problems. The grid voltage, converter side potential, as well as grid current from the synchronous reference frame in this instance are represented by the *d-q* elements U_{dq}, V_{dq}, and i_{dq}, respectively. The U_{dq} equation is represented by Eq. (5). Eq. (6) provides the discrete state space formula of the network.

$$U_{dq}=V_{dq}+R\cdot i_{dq}+L_f\cdot\frac{di_{dq}}{dt} \tag{5}$$

$$x\left(k+1\right)=A\cdot x\left(k\right)+B\cdot u\left(k\right)+M \tag{6}$$

Eq. (7) represents the state variable *x*, and the subsequent Eqs. (8) to (11) represent other System parameters.

$$x=\left[i_d,i_q\right]^T \tag{7}$$

$$u=\left[V_d,V_q\right]^T \tag{8}$$

$$A=\begin{bmatrix}\left(1-\dfrac{T_sR}{L_f}\right) & T_s\omega\\ -T_s\omega & \left(1-\dfrac{T_sR}{L_f}\right)\end{bmatrix} \tag{9}$$

Input Matrix,

$$B=\left[-\frac{1}{L_f},-\frac{1}{L_f}\right] \tag{10}$$

$$M=\left[\frac{u_d}{L_f},\frac{u_q}{L_f}\right] \tag{11}$$

To find the real and reactive powers of the $(k+2)^{th}$ position at PCC, utilize Eq. (12).

$$\begin{bmatrix} P(k+2) \\ Q(k+2) \end{bmatrix} = \begin{bmatrix} \left(1-\frac{T_s R}{L_f}\right) & T_s\omega \\ -T_s\omega & \left(1-\frac{T_s R}{L_f}\right) \end{bmatrix} \begin{bmatrix} P(k+1) \\ Q(k+1) \end{bmatrix} + \frac{T_s}{L_f} \begin{bmatrix} U_d(k+2)\cdot V_d(k+1) - V_d^2(k+1) \\ -U_q(k+2)\cdot V_q(k+1) \end{bmatrix} \tag{12}$$

In the next control cycle, the switching condition related to the vector voltages that produces the minimum value of the predefined objective function will be chosen and applied to the converter.

3.3 MPCP Control Model

The battery is discharged by using the lower output voltage that the buck-boost converter produces from the lower input voltage. There can be just two possible values for the current i_b in boost mode, as indicated beneath in Eqs. (13) and (14).

$$L_b \frac{di_b}{dt} = V_b \tag{13}$$

$$L_b \frac{di_b}{dt} = V_b - V_{dc} \tag{14}$$

The discrete-time model for a sampling Period ts is expressed in Eq. (15) and Eq. (16).

$$i_b(k+1) = \frac{t_s}{L_b} V_b(k) + i_b(k) \tag{15}$$

$$i_b(k+1) = \frac{t_s}{L_b}\left(-V_{dc}(k) + V_b(k)\right) + i_b(k) \tag{16}$$

Eq. (17) illustrates how a cost function could be developed to control battery current whether it has been charged or discharged.

$$C_v = \left| i_b^* - i_b(k+1) \right| \tag{17}$$

The $(k + 1)^{th}$ power necessitated by BESS to hold the micro grid's power balance shall then be evaluated using Eq. (18).

$$p_b^*(k+1) = \left| i_{dc}(k+1) * V_{dc}^* \right| \tag{18}$$

Given that the battery voltage V_b changes relatively slowly and that the inductor current I_b and battery current outflow i_{bat} are equivalent in steady state, it is possible to forecast the battery output power P_O by using Eq. (19).

$$P_O(k+1) = \left| i_b(k+1) * V_b(k) \right| \tag{19}$$

It is feasible to predict the battery's output power as follows given that the battery voltage V_b fluctuates relatively slowly and that, in a steady state, the inductor current I_b and the battery current discharge i_{bat} are equal.

$$C_p = \left| P_b^*(k+1) - P_O(k+1) \right| \tag{20}$$

The switching mode of the buck-boost converter is selected such that the cost function in Eq. (20) is minimised.

3.4 MPVP Control Algorithm

The capacitor filter potential is predicted using the current output, and each sampling period's switching state is ascertained by minimalizing a cost function. The discrete-time equation will be used to predict the expected output current and capacitor filter voltage for various voltage vector V_k evaluates at the time of $(j + 1)$.

$$i(j+1) = i(j) + \frac{T_{sp}}{L}\left[V(j) - V_c(j) - R_c\left(i(j) - i_g(j)\right)\right] \tag{21}$$

The projected capacitor potential at the $(j + 1)^{th}$ moment can be expressed as follows by converting Eq. (21) into Eq. (22).

$$V_c(j+1) = V_C(j) + \frac{T_{sp}}{C}\left[i(j+1) - i_g(j)\right] \tag{22}$$

$$V_c(j+1) = V_c(j) + \frac{T_{sp}}{C}\left[i(j) + \frac{T_{sp}}{L}\left[V(j) - V_c(j) - R_c\left(i(j) - i_g(j)\right)\right] - i_g(j)\right] \tag{23}$$

Once voltage $V_c((j + 1))$ were calculated and related with the help of a cost variable g, the ideal voltage vector $V(j)$ that minimalizes Eq. (23) is chosen and employed at the subsequent sampling time.

4 SIMULATION OUTCOMES AND ANALYSES

For the suggested design, a MATLAB/Simulink model has been utilized to model and analyze the recommended Fuzzy based DMPPC, MPVP, MPCP, and SMC, controllers. The analysis's conclusions are given. Twelve solar PV modules of 64.2 V capacity, a power of 305 W, and a current rating of 5.96 A were assumed for the simulation purposes. A wind farm having a wind speed of 11 m/s^2, power rating of 500 W and voltage rating of 250 V are considered for simulation purposes. Tab. 1 comprises the simulation parameters.

Table 1 Ratings of the variables considered

Name of Variable	Rating
FilterCircuit inductance L	0.09 H
Filter Circuit capacitor C	100 µF
DC voltage	220 V
Load Resistance	$R = 30$ ohm
Sampling instance	20 µs

The output voltage and current waveforms for the WECS are shown in Fig. 4 before and after the AC-DC converter.

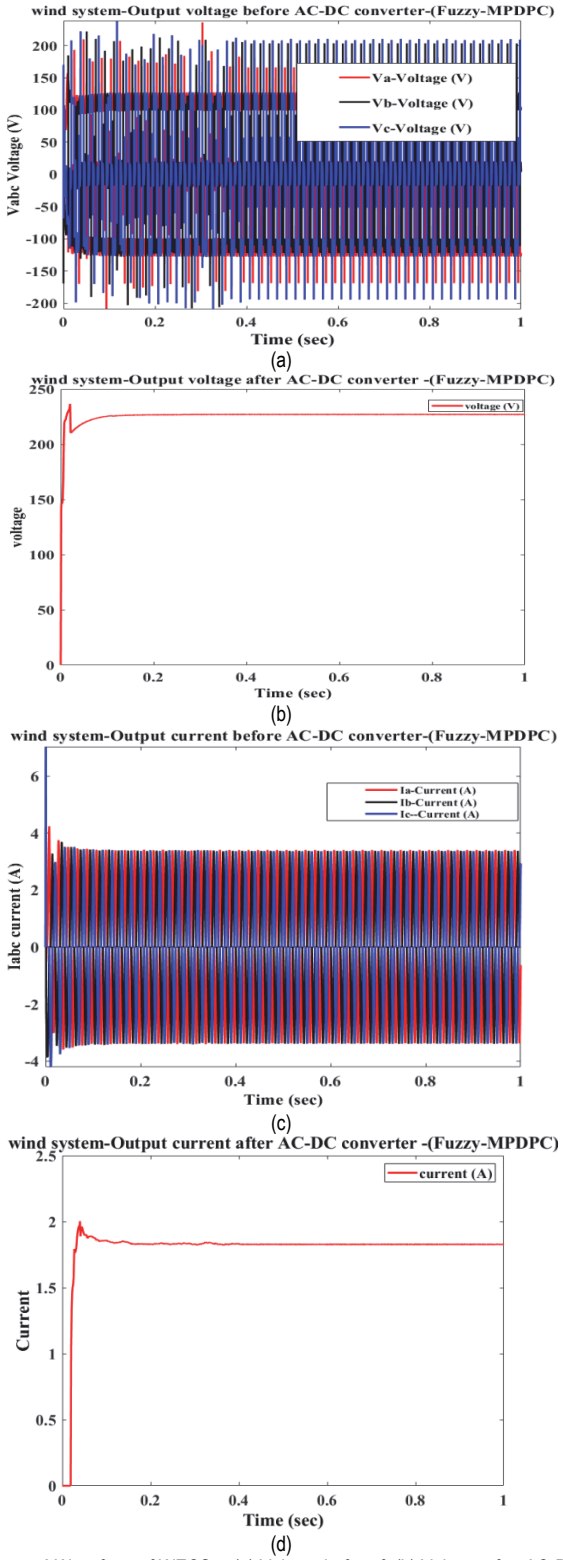

Figure 4 Waveform of WECS's: (a) Voltage before & (b) Voltage after AC-DC converter (c) Current before and (d) Current after AC-DC converter

The solar system's output voltage and current waveforms are shown in Fig. 5.

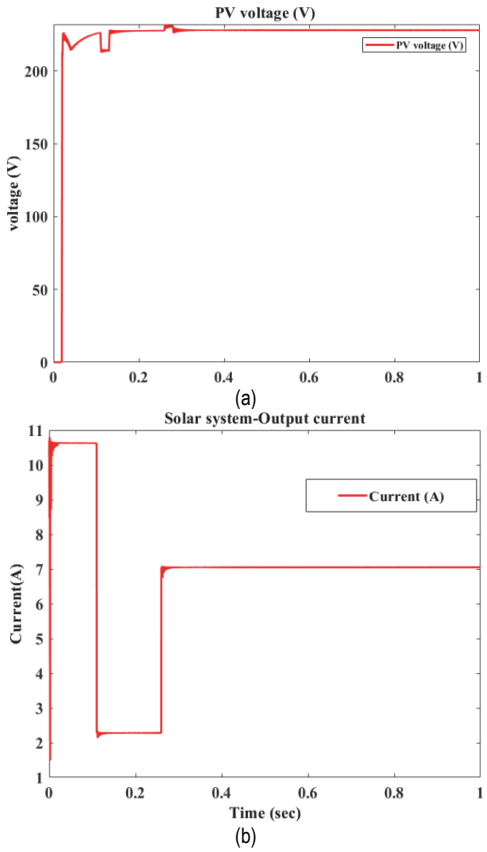

Figure 5 Solar system output: (a) Voltage and (b) Current

The voltage output of the DC/DC converter before and after the filtering circuit is shown in Fig. 6 and clearly illustrates how much the ripple content in the waveform is diminished through the assistance of the filter.

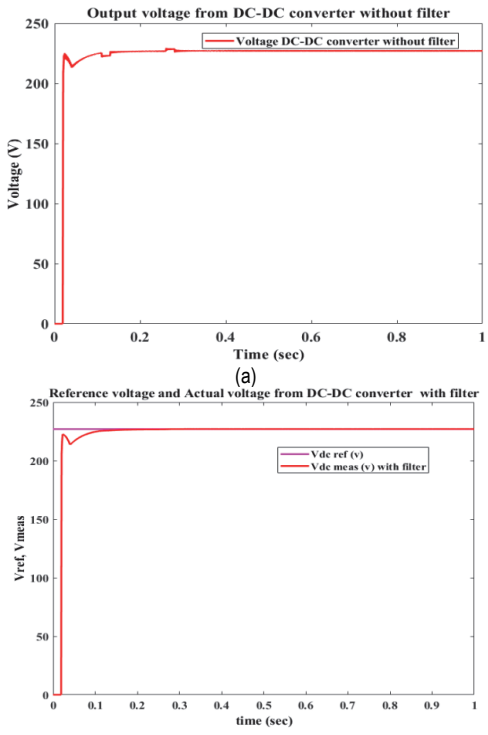

Figure 6 Voltage output of a DC to DC configuration: (a) Without filter & (b) With filter

Fig. 7 shows the current, power and capacitor link voltage at the PCC of the system for the suggested controller. It also depicts the voltage across the filter capacitance of the system for the suggested controller.

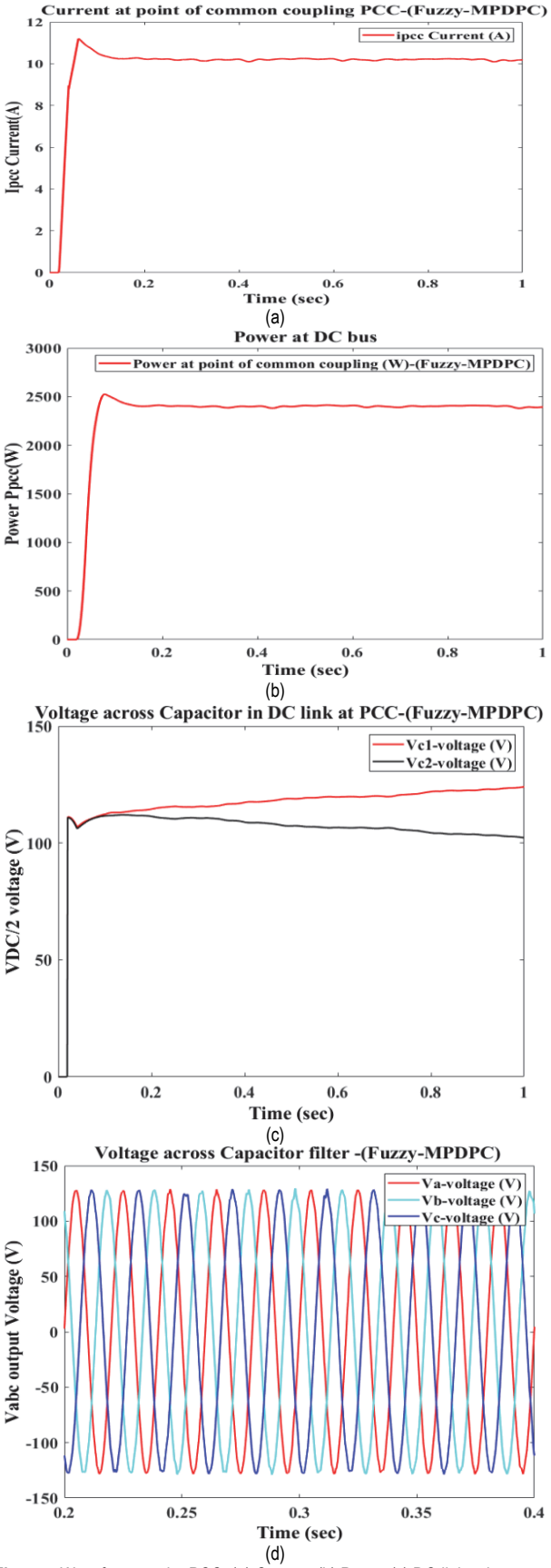

Figure 7 Waveforms at the PCC: (a) Current, (b) Power (c) DC-link voltage and (d) capacitor filter voltage

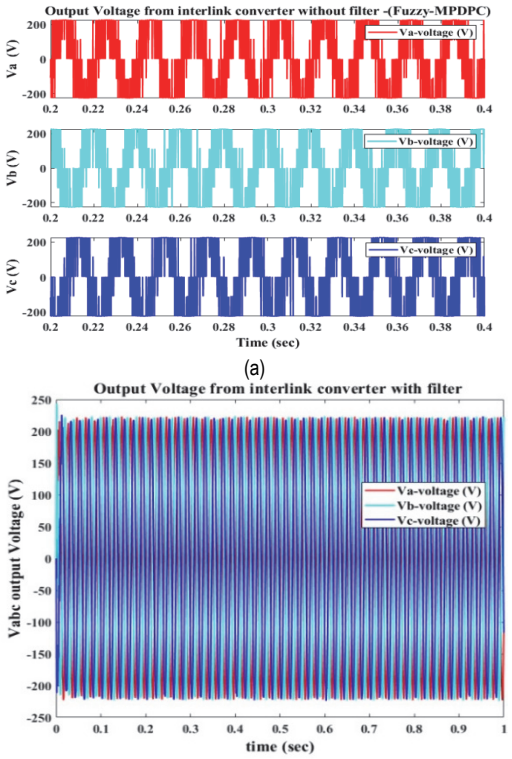

Figure 8 Interlink converter: (a) Output voltage without filter & (b) With filter

The voltage across the interlink converter of the 3 phases, namely $V_a, V_b, \& V_c$ are displayed in Fig. 8 respectively and show the potential across the recommended interlink converter excluding and including filters. It is clear from this figure, that ripple is notably condensed by the filter design of the converter.

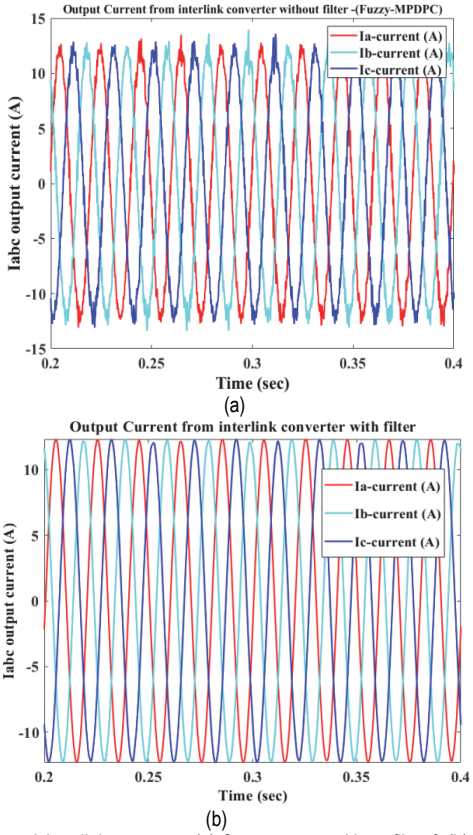

Figure 9 Interlink converter: (a) Output currentwithout filter & (b) With filter

Similarly, Fig. 9 depicts the interlink converter's output current waveforms with & without filter. It also clearly shows the current ripple is notably reduced by the filter design of the converter. Fig. 10 and Fig. 11 display the comparison of the various parameters, that shows the robustness and efficacy of the proposed controller.

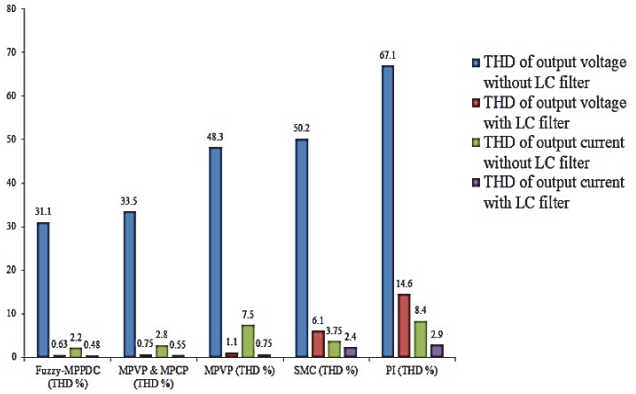

Figure 10 Comparison of THD % of voltage for all controllers

Fig. 10 shows the THD comparison chart of the different controllers with and without filters. It can be clearly witnessed that the proposed Fuzzy-MPPDC controller is superior to the other types.

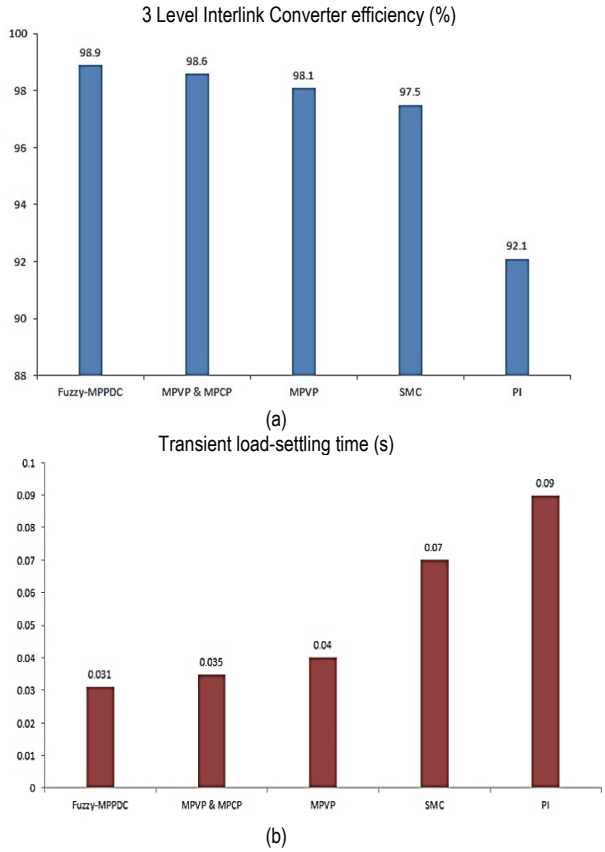

Figure 11 Comparison of (a) Efficiency & (b) Transient load settling time for all controllers

Fig. 11 depicts the efficiency and the transient settling times for the various controllers. Again the dominance of the recommended method can be noted.

Tabs. 2 to 5 provide an overview of the simulation results. Tab. 2 shows the output voltage and current total harmonic distortion (THD) percentage for each type of controller, both with and without filters.

Table 2 Comparison of % THD for all types of controllers

During Load	THD of output voltage without LC filter	THD of output voltage with LC filter	THD of output current without LC filter	THD of output current with LC filter
Fuzzy-MPPDC (THD %)	31.1	0.63	2.2	0.48
MPVP & MPCP (THD %)	33.5	0.75	2.8	0.55
MPVP (THD %)	48.3	1.1	7.5	0.75
SMC (THD %)	50.2	6.1	3.75	2.4
PI (THD %)	67.1	14.6	8.4	2.9

Tab. 3 presents the % THD for all types of controllers under tested load conditions.

Table 3 THD (%) Comparison for types of controllers under tested load conditions

Load Condition	% THD Output Voltage Comparison with LC Filter				
	DMPPC	MPVP	MPCP	SMC	PI
Light load (20-30%)	0.63	0.75	1.1	6.1	14.6
Medium load (50-60%)	2.3	2.9	3.1	7.2	16.3
Heavy Load (80-100%)	3.1	3.8	4.0	8.1	17.2

A summary of each controller's converter efficiency as well as settling time under transient circumstances can be found in Tab. 4.

Table 4 Converter efficiency & settling times for all types of controllers

During Load	Fuzzy-MPPDC	MPVP & MPCP	MPVP	SMC	PI
3 Level Interlink converter efficiency / %	98.9	98.6	98.1	97.5	92.1
Transient load - settling time / s	0.031	0.035	0.04	0.07	0.09

Tab. 5 represents the comparison of settling times for various controllers under tested load conditions.

Table 5 Settling times for all types of controllers under tested load conditions

Load Condition	Settling Time Comparison				
	DMPPC	MPVP	MPCP	SMC	PI
Light (20-30% load)	0.031	0.035	0.04	0.07	0.11
Medium (50-60% load)	0.12	0.15	0.18	0.23	0.29
Heavy (80-100% load)	0.19	0.25	0.29	0.31	0.38

5 CONCLUSIONS

In conclusion, this research presents the successful design, simulation, and verification of a novel Fuzzy-Based Direct Model Predictive Power Control (Fuzzy-DMPPC) system for managing a hybrid grid-connected network utilizing a three-stage AC/DC interlinking converter. The proposed controller addresses the limitations of conventional DMPPC by incorporating fuzzy logic-based decision-making into the objective function, enabling adaptive and intelligent responses to

dynamic system conditions. Unlike traditional MPC approaches that rely heavily on complex optimization and linear modeling, the Fuzzy-DMPPC framework utilizes basic mathematical formulations, significantly reducing computational complexity and enhancing real-time applicability. Moreover, the proposed cost function, enhanced with fuzzy logic, adaptively adjusts weights based on SOC and RES conditions, enabling real-time prioritization, smoother operation, and improved robustness over traditional predictive controllers. Simulation results confirm the superior performance of the proposed control system across multiple key metrics. The Total Harmonic Distortion (THD) of voltage was minimized to an impressive 0.63%, outperforming all other evaluated controllers. Furthermore, the proposed Fuzzy-DMPPC improved converter efficiency to 98.9%, demonstrating its capability in enhancing energy conversion quality. The findings validate that the Fuzzy-DMPPC system can effectively regulate the bidirectional flow of power in the battery energy storage system (BESS), while ensuring stable AC voltage output and seamless power exchange between the microgrid and the utility grid. These outcomes establish the proposed controller as a highly efficient, intelligent, and robust solution for advanced power management in hybrid renewable energy systems, paving the way for practical implementation in smart grid applications and sustainable energy infrastructures.

5 REFERENCES

[1] Moghadasi, A., Sargolzaei, A., Anzalchi, A., Moghaddami, M., Khalilnejad, A., & Sarwat, A. (2017). A model predictive power control approach for a three-phase single-stage grid-tied PV module-integrated converter. *IEEE Transactions on Industry Applications*, *54*(2), 1823-1831. https://doi.org/10.1109/TIA.2017.2787626

[2] Xing, X., Zhang, C., He, J., Chen, A., & Zhang, Z. (2017). Model predictive control for parallel three-level T-type grid-connected inverters in renewable power generations. *IET Renewable Power Generation*, *11*(11), 1353-1363. https://doi.org/10.1049/iet-rpg.2016.0361

[3] Wu, D., Liang, S., Chen, C., Chen, Y., Wang, P., & Long, Z. (2024). Power load forecasting based on LSTM deep learning algorithm. *Tehnički vjesnik - Technical Gazette*, *31*(6), 2156-2160. https://doi.org/10.17559/TV-20230708000790

[4] Dong, H., Xu, Z., Song, P., Tang, G., Xu, Q., & Sun, L. (2017). Optimized power redistribution of offshore wind farms integrated VSC-MTDC transmissions after onshore converter outage. *IEEE Transactions on Industrial Electronics*, *64*, 8948-8958. https://doi.org/10.1109/TIE.2016.2631136

[5] Dharmasena, S., & Choi, S. (2019). Model predictive control of five-phase permanent magnet-assisted synchronous reluctance motor. *Proceedings of the 2019 IEEE Applied Power Electronics Conference and Exposition (APEC)*, 1885-1890. https://doi.org/10.1109/APEC.2019.8721887

[6] Han, Y., Li, H., Shen, P., Coelho, E., & Guerrero, J. M. (2017). Review of active and reactive power sharing strategies in hierarchical controlled microgrids. *IEEE Transactions on Power Electronics*, *32*(3), 2427-2451. https://doi.org/10.1109/TPEL.2016.2569597

[7] Ang, K. H., Chong, G., & Li, Y. (2014). PID control system analysis, design, and technology. *IEEE Transactions on Control Systems Technology*, *13*(5), 1813-1827. https://doi.org/10.1109/TCST.2005.847331

[8] Shadmand, M. B., Li, X., Balog, R. S., & Abu-Rub, H. (2017). Constrained decoupled power predictive controller for a single-phase grid-tied inverter. *IET Renewable Power Generation*, *11*(5), 659-668. https://doi.org/10.1049/iet-rpg.2016.0520

[9] Dong, H., Xu, Z., Song, P., Tang, G., Xu, Q., & Sun, L. (2017). Optimized power redistribution of offshore wind farms integrated VSC-MTDC transmissions after onshore converter outage. *IEEE Transactions on Industrial Electronics*, *64*, 8948-8958. https://doi.org/10.1109/TIE.2016.2631136

[10] Kumar, P. S. S., Lenine, D., Kiran, P. S., Tummala, S. K., Al-Jawahry, H. M., & Singh, S. (2023). Energy management system for small-scale hybrid wind solar battery-based microgrid. *E3S Web of Conferences*, *391*, 01138. https://doi.org/10.1051/e3sconf/202339101138

[11] Han, H., Hou, X., Yang, J., Wu, J., Su, M., & Guerrero, J. M. (2016). Review of power sharing control strategies for islanding operation of AC microgrids. *IEEE Transactions on Smart Grid*, *7*(1), 200-215. https://doi.org/10.1109/TSG.2015.2434849

[12] Chaiyatham, T. & Ngamroo, I. (2017). Improvement of power system transient stability by PV farm with fuzzy gain scheduling of PID controller. *IEEE Systems Journal*, *11*(3), 1684-1691. https://doi.org/10.1109/JSYST.2014.2347393

[13] Liu, Z., Miao, S., Wang, W., & Sun, D. (2021). Comprehensive control scheme for an interlinking converter in a hybrid AC/DC microgrid. *CSEE Journal of Power and Energy Systems*, *7*(4), 719-729.

[14] Benadli, R., Bjaoui, M., Khiari, B., & Sellami, A. (2021). Sliding mode control of hybrid renewable energy system operating in grid-connected and stand-alone mode. *Power Electronics and Drives*, *6*(41), 41-52. https://doi.org/10.2478/pead-2021-0012

[15] Kayalvizhi, S. & Kumar, D.M.V. (2017). Load frequency control of an isolated microgrid using fuzzy adaptive model predictive control. *IEEE Access*, *5*, 16241-16251. https://doi.org/10.1109/ACCESS.2017.2735545

[16] Liu, X., Wang, D., & Peng, Z. (2019). Cascade-free fuzzy finite-control-set model predictive control for nested neutral point-clamped converters with low switching frequency. *IEEE Transactions on Control Systems Technology*, *27*(5), 2237-2244. https://doi.org/10.1109/TCST.2018.2839091

[17] Wang, B., Yang, L., Wu, F., & Chen, D. (2019). Fuzzy predictive functional control of a class of non-linear systems. *IET Control Theory Applications*, *13*(14), 2281-2288. https://doi.org/10.1049/iet-cta.2018.5903

[18] Liu, X., Wang, D., & Peng, Z. (2019). Cascade-free fuzzy finite-control-set model predictive control for nested neutral point-clamped converters with low switching frequency. *IEEE Transactions on Control Systems Technology*, *27*(5), 2237-2244. https://doi.org/10.1109/TCST.2018.2839091

[19] Hu, J., Xu, Y., Cheng, K. W., & Guerrero, J. M. (2018). A model predictive control strategy of PV-battery microgrid under variable power generations and load conditions. *Applied Energy*, *221*, 195-203. https://doi.org/10.1016/j.apenergy.2018.03.128

[20] Kumari, J. S., Babu, C. S., & Lenine, D. (2010). Evolutionary computing-based multilevel H-bridge cascaded inverter with photovoltaic system. *Proceedings of the 2010 International Conference on Advances in Recent Technologies in Communication and Computing*, 121-125. https://doi.org/10.1109/ARTCom.2010.46

[21] Priyanka, G., Kumari, J. S., Lenine, D., Tummala, S. K., Al-Jawahry, H. M., & Gupta, H. (2023). Reduced common mode multilevel inverter strategy in photovoltaic systems. *E3S Web of Conferences*, *391*, 01136. https://doi.org/10.1051/e3sconf/202339101136

[22] Panchanathan, S., Vishnuram, P., Rajamanickam, N., Bajaj, M., Blazek, V., Prokop, L., & Misak, S. (2023). A

comprehensive review of the bidirectional converter topologies for the vehicle-to-grid system. *Energies*, *16*(5), 2503. https://doi.org/10.3390/en16052503

[23] Ma, T., Cintuglu, M. H., & Mohammed, O. A. (2017). Control of hybrid AC/DC microgrid involving energy storage and pulsed loads. *IEEE Transactions on Industry Applications*, *53*(1), 567-575. https://doi.org/10.1109/TIA.2016.2613981

[24] Kumar, P. S. S., Suresh, P., & Lenine, D. (2024). Performance improvement of predictive voltage control for interlinking converters of integrated microgrid. *Measurement: Sensors*, *33*, 101196. https://doi.org/10.1016/j.measen.2024.101196

[25] Kumari, J. S., Babu, C. S., Lenine, D., & Lakshman, J. (2009). Improvement of static performance of multilevel inverter for single-phase grid-connected photovoltaic modules. *Proceedings of the 2009 Second International Conference on Emerging Trends in Engineering & Technology*, 691-697. https://doi.org/10.1109/ICETET.2009.61

[26] Shan, Y., Hu, J., Chan, K. W., Fu, Q., & Guerrero, J. M. (2018). Model predictive control of bidirectional DC-DC converters and AC/DC interlinking converters - A new control method for PV-wind-battery microgrids. *IEEE Transactions on Sustainable Energy*, *9*(4), 1190-1199. https://doi.org/10.1109/TSTE.2018.2873390

Contact information:

P. SAI SAMPATH KUMAR
(Corresponding author)
1) Department of Electrical and Electronics Engineering,
SRM Institute of Science and Technology, Kattankulathur, Chennai 603203
2) RGM College of Engineering & Technology, Nandyal,
Andhra Pradesh, India 518501
E-mail: sammitsme@gmail.com

P. SURESH
Department of Electrical and Electronics Engineering,
SRM Institute of Science and Technology,
Kattankulathur, Chennai 603203, India
E-mail: suresh.au95@gmail.com

D. LENINE
Department of Electrical and Electronics Engineering,
RGM College of Engineering & Technology,
Nandyal, Andhra Pradesh, India 518501
E-mail: lenine.eee@gmail.com